Reelin protects from colon pathology by maintaining the intestinal barrier integrity and repressing tumorigenic genes

Ana E. Carvajal, José M. Serrano-Morales, María D. Vázquez-Carretero, Pablo García-Miranda*, María L. Calonge, María J. Peral and Anunciación A. Ilundain

Departamento de Fisiología, Facultad de Farmacia, Universidad de Sevilla, Spain.

Short title: Reelin protects from colon pathology

Ana E. Carvajal and José M. Serrano-Morales contributed equally to this work.

*Corresponding author: Dr. P García-Miranda

Depto. Fisiología, Facultad de Farmacia, Universidad de Sevilla

C/ Profesor García González, nº 2

41012 Sevilla, Spain.

Telephone: 34 954556357

Email: pgarcia2@us.es

ABSTRACT

We previously reported that reelin, an extracellular matrix protein first known for its key role in neuronal migration, reduces the susceptibility to dextran sulphate sodium (DSS)-colitis. The aim of the study was to determine whether reelin protects from colorectal cancer and how reelin defends from colon pathology. In the colon of wild- type and of mice lacking reelin (reeler mice) we have analyzed the: i) epithelium cell renewal processes, ii) morphology, iii) Sox9, Cdx2, Smad5, Cyclin D1, IL-6 and IFNγ mRNA abundance in DSS-treated and untreated mice, and iv) development of azoxymethane/DSS-induced colorectal cancer, using histological and real time-PCR methodologies. The reeler mutation increases colitis-associated tumorigenesis, with increased tumours number and size. It also impairs the intestinal barrier because it reduces cell proliferation, migration, differentiation and apoptosis; decreases the number and maturation of goblet cells, and expands the intercellular space of the desmosomes. The intestinal barrier impairment might explain the increased susceptibility to colon pathology exhibited by the reeler mice and is at least mediated by the down-regulation of Sox9 and Cdx2. In response to DSS-colitis, the reeler colon increases the mRNA abundance of IL-6, Smad5 and Cyclin D1 and decreases that of IFNγ, conditions that might result in the increased colitis-associated tumorigenesis found in the reeler mice. In conclusion, the results highlight a role for reelin in maintaining intestinal epithelial cell homeostasis and providing resistance against colon pathology.

Keywords: reelin**,** colitis, cancer

1. Introduction

The intestinal epithelium provides a protective barrier against a broad spectrum of potentially lethal microorganisms and carcinogens that are present in the intestinal lumen. From the outer to the inner layer, the intestinal barrier is composed of gut microbiota; a mucus layer secreted by goblet cells, especially thick in the colon, that contains antimicrobial peptides and IgA; epithelial cells with its paracellular pathway sealed, and the innate and adaptive immune cells [1]. The epithelium is the foremost component of the intestinal barrier and its rapid and controlled cell turnover allows to adjust the cell renewal processes in response to intrinsic and extrinsic signals and to maintain the integrity of the barrier. The epithelial cells are constantly generated from multipotential stem cells located in the crypts. The progeny cells differentiate as they move up to the surface epithelium and eventually they are released into the intestinal lumen with a turnover time of 4 to 6 days. In the colon, the three main types of differentiated cells are colonocytes, that have both absorptive and secretory functions; goblet cells that secret a variety of factors, including proteins, trefoil factors and mucins, all of which help to protect the mucosa from injury, and enteroendocrine cells that secrete hormones that regulate gastrointestinal function [2]. Deregulation of epithelial homeostasis, such as perturbations in the balance between cell production, differentiation and shedding, compromises the epithelial barrier function and if the integrity of the barrier is not re-established, intestinal disorders such as inflammatory diseases, malignant tissue transformation and cancer could occur (see [1] for a recent review).

In spite of the number of studies regarding colon epithelium homeostasis, the molecular mechanisms involved in such process and in those modified under pathological conditions are not precisely understood. Normal homeostasis requires a cross talk between the epithelium and mesenchymal cells, being the pericryptal myofibroblasts one of the most important sources of factors that regulate epithelium renewal processes. The synthesis and secretion of various substances as well as their expression of receptors for many of these substances, allow the myofibroblasts to orchestrate functions that ranged from the control of epithelial cell renewal and wound repair to participation in the underlying pathophysiology that characterizes ulcerative colitis and colorectal cancer [3]. In addition, its strategic location between the epithelium and mucosa immune system allows their direct interaction with antigens that cross the epithelial barrier.

We previously reported that the subepithelial myofibroblasts of rodent small [4,5] and large intestine [6] and of human colon [7] express reelin, an extracellular matrix protein that was first known by its function in brain development [8]. More recently we

reported that the mice colon responds to DSS-treatment up-regulating reelin and that the absence of reelin (reeler mutation) exacerbates DSS-induced colitis phenotype [6], suggesting that reelin protects from colon pathology.

The purpose of the present work was to determine whether reelin protects from colon cancer development and to understand how reelin provides resistance against colon pathology. We have used the colon of wild-type and reeler mice and examined the consequences of reelin absence on: 1) epithelium homeostasis, morphology and gene expression in DSS-treated and untreated animals and 2) tumour development in response to azoxymethane/dextran sodium sulphate (AOM/DSS)-treatment.

Preliminary reports of some of these results were published as abstracts [9–11].

2. Materials and methods

2.1. Materials

The antibodies: anti-cleaved caspase-3 (Asp175) was obtained from Cell Signaling, anti-BrdU (B2531) from Sigma-Aldrich, anti-Muc2 (Sc15334) and anti-carbonic anhydrase-1 from Santa Cruz Biotechnology, Inc., and anti-chromogranin A (NB120-15160) from Novus Biologicals. Biotinylated peroxidase-conjugated anti-mouse and anti-rabbit IgG were obtained from Sigma-Aldrich. Unless otherwise stated, the other reagents were obtained from Sigma-Aldrich, Spain.

2.2. Animals

Male and female wild-type and reeler mice (B6C3Fe) of one and three month-old were used. Reeler (*rl*) mice have a spontaneous autosomal recessive mutation of reelin [8]. Heterozygous (rl^+/rl^-) mice were purchased from Jackson Laboratories (Bar Harbor, ME), through Charles River Laboratories, Spain. Wild-type (rl^+/rl^+) and homozygous reeler (rl^-/rl^-) mice were obtained by heterozygous crossings. The animals were housed in a 12:12 light-dark cycle and fed *ad libitum* with Global 2019 extruded rodent diet (Harlan Ibérica S.L.) with free access to tap water. Mice were genotyped by PCR analysis of genomic DNA as described [6]. The mice were humanely handled and sacrificed by cervical dislocation in accordance with the guidelines of the European Union Council (Directive 2010/63/UE) concerning the protection of experimental animals.

2.3. Experimental design

Epithelium homeostasis measurements (cell proliferation, migration, differentiation and apoptosis) and morphological studies were performed in the absence of experimental-induced colon pathology.

Acute colitis was induced as previously described [6]. Briefly, three month-old wild-type and reeler mice were randomized into untreated and DSS-treated groups, which received either water or water containing 3% (wt/vol) DSS (40 kDa, TdB Consultancy, Uppsala, Sweden), respectively, during 9 days. Fresh DSS solution was provided every day. Daily, throughout the DSS-treatment, body weight, stool consistency and presence of blood in feces were recorded to follow colitis development. Following sacrifice, the murine colon was removed, opened longitudinally, washed with ice-cold saline solution and subdivided into proximal and distal regions. For PCR-measurements tissues were frozen at -80ºC until used.

Tumours were induced on three month-old wild-type and reeler mice by AOM/DSS, following the protocol of Okayasu et al [12]. DSS-treatment induces chronic

colitis and the AOM accelerates tumorigenesis. A single intraperitoneal dose of 10 mg of AOM per kg body weight was injected and 7 days later 1% (wt/vol) DSS was administered in the drinking water during 4 days, followed by 14 days with tap water. The DSS/tap water cycle was repeated three times. The clinical parameters described above were recorded daily during the DSS-treatment. Following sacrifice, the colon was removed and examined for the presence of tumours. The tumours were counted, their diameter measured and removed from the colon by micro-dissection.

2.4. Immunostaining analysis

0.5 cm colon segments that were incubated in phosphate-buffered saline (PBS) containing 4% paraformaldehyde at 4°C overnight. Immunostaining assays were performed on either 7 µm cryosections or 5 µm paraffin-embedded sections of intact colon as previously described [5]. The slides containing the colon sections were incubated with the indicated primary antibody at 4ºC, overnight. Antibody binding was visualized with biotinylated anti IgG antibodies, at dilution 1:100, followed by immunoperoxidase staining. The Vectastain ABC peroxidase kit (Vector) and 3,3'-diaminobenzidine were used. Controls were carried out without primary antibody. The slides were rinsed, mounted and photographed with a Zeiss Axioskop 40 microscope equipped with a SPOT Insight V 3.5 digital camera. Acquired images were analysed by using Spot Advance 3.5.4.1 program (Diagnostic Instrument, Inc). The magnification was 20x10.

2.5. Measurement of cell proliferation and migration rate

Epithelial cell proliferation and migration rates were quantified by measuring the incorporation of 5-bromo deoxyuridine (BrdU) into DNA. Mice received an intraperitoneal injection of BrdU (120 mg/Kg body weight) and were killed either 90 min or 15 h later for either epithelial cell proliferation or migration measurements, respectively. Colon sections were processed for immunohistochemistry and BrdU staining was detected with a monoclonal anti-BrdU antibody, 1:300 dilution, as previously [5]. The number of labelled cells in 30 longitudinally well oriented crypts per mouse was determined by light microscopy. Epithelial cell proliferation is expressed as the number of BrdU-positive cells per crypt. The cell migration rate is estimated by measuring the distance from the base of the crypt to the foremost-labelled cell and expressed as µm/h.

2.6. Measurement of cell apoptosis

The apoptotic cells in the colon epithelium were identified and quantified by immunohistochemistry assay of cleaved caspase-3. A polyclonal anti-cleaved caspase-3 antibody was used at dilution 1:200. The number of labelled cells in 150 longitudinally

well oriented crypts per mouse was determined by light microscopy. Results are expressed as the number of labelled cells per 10 crypts.

2.7. Measurement of cell differentiation

Alcian Blue, Periodic Acid-Shiff (PAS) and the anti-Muc2 antibody (1:25 dilution) were used to stain acidic, neutral and Muc2 mucins, respectively. Colonocytes and enteroendocrine cells were identified by immunohistochemical detection of carbonic anhydrase-1 and chromogranin A, respectively. The number of labelled cells was determined in at least 30 crypts longitudinally well oriented per mouse. Results are expressed as the number of labeled cells per crypt.

2.8. Morphological studies

The tissues were incubated in phosphate-buffered saline (PBS) containing 4% paraformaldehyde at 4°C overnight. Paraffin-embedded sections (5 μm) of proximal and distal colon, obtained from wild-type and reeler mice, were stained with hematoxylin and eosin procedure. Measurements of the diameter and depth of the crypts were done on at least 30 well oriented, full-length crypts. Morphometric measurements of the crypts and tumours were performed by Spot Advance 3.5.4.1. images analysis program (Diagnostic Instrument, Inc.).

2.9. Electron microscopy studies

Segments of distal colon were fixed in 4% glutaraldehyde/0.1 mol/L sodium cacodylate, pH 7.4 at 4ºC for 3 h. After three rinses in cacodylate-buffered solution, the tissues were postfixed in 1% OsO_4 in 0.1 M phosphate buffer at 4ºC for 1 h and washed in cacodylate-buffered solution containing 7.5% sucrose. The segments were then dehydrated in a graduated series of acetone (30%, 50% and 70%), stained with 2% uranyl acetate and embedded in Spurr's epoxy resin. Ultrathin sections (80-100 nm) were examined under a Philips CM-10 transmission electron microscope equipped with an Olympus Veleta camera. The photographs were processed with iTEM software and ImageJ program version 1.46 (National Institutes for Health, http://rsb.info.nih.gov/ij/index.html).

2.10. Relative quantification of Real-time PCR

Total RNA was extracted from the colon using RNeasy® kit (Qiagen, Hilden, Germany). RNA purity was assessed by spectrophotometry measurements of $OD_{260/280}$ and its integrity by visual inspection after electrophoresis on an agarose gel in the presence of RedSafe™ (Intron Biotechnology) nucleic acid staining. cDNA was synthesized from 1 μg of total RNA using QuantiTect® reverse transcription kit (Qiagen) as described by the manufacturer. The primers used are given in Table 1.

Real-time PCR was performed with 10 µl SsoFast™ EvaGreen® Supermix (BioRad), 0.4 µM primers and 1 µl cDNA. Controls were carried out without cDNA. Amplification was run in a MiniOpticon™ System (BioRad) thermal cycler (95 °C /3 min; 35 cycles of 94 °C /40 s, 58 °C/ 40 s and 72 °C/ 40 s, and 72 °C /2 min). Following amplification, a melting curve analysis was done by heating the reactions from 65 to 95 °C in 1 °C intervals while monitoring fluorescence. Analysis confirmed a single PCR product at the predicted melting temperature. β-Actin served as reference gene and was used for samples normalization. The cycle at which each sample crossed a fluorescence threshold, Ct, was determined and the triplicate values for each cDNA were averaged. Analyses of PCR were done using the comparative Ct method with the Gene Expression Macro software supplied by BioRad.

2.11. Statistical analysis

Data are presented as mean ± SEM. Comparisons between different experimental groups were evaluated by the two-tailed Student's t-test. One-way ANOVA followed by the Newman-Keuls´ test was used for multiple comparisons (GraphPad Prism program). Differences were set to be significant for $p<0.05$.

3. Results

3.1. Absence of reelin and the homeostasis of the colon epithelium

To test whether the increased susceptibility of the reeler mice to DSS-colitis was associated with epithelial barrier defects, we first determined whether reelin contributes to the homeostasis of the crypt/surface axis of the colon. This was achieved by evaluating the cell proliferation, migration, differentiation and apoptosis of proximal and distal colon epithelium of 1 month-old wild-type and reeler mice.

BrdU incorporation into DNA was measured to determine the effects of the reeler mutation on epithelial cell proliferation and migration rates, as described in Methods. The results show that at 90 min after injection, BrdU is mainly observed in the nuclei of the cells located in the first third of the crypts of both types of mice (Fig. 1A). At 15 h after the injection, the BrdU positive cells occupy nearly the full length of the crypt in the wild-type mice, but only the lower half of the crypts in the reeler mice (Fig. 1B). The quantification of the marked nuclei reveals that in the wild-type mice the cell proliferation and migration rates are greater in the distal than in the proximal colon and that the mutation significantly decreases cell proliferation (by 47.5 ± 4.9% and 55 ± 3.2% in proximal and distal colon, respectively) and migration (by 33 ± 3.2% and 20.4 ± 2.4% in proximal and distal colon, respectively).

Cell apoptosis, evaluated by immunological detection of cleaved caspase-3, is only observed at the surface epithelium in both types of mice and colon segments. In wild-type mice, the number of apoptotic cells is higher in the distal than in the proximal colon and the reeler mutation significantly decreases the number of apoptotic cells in the distal colon (Fig. 1C). The mutation does not significantly affect apoptosis in the proximal colon.

Cell differentiation into goblet cells was evaluated by detection of acid (Alcian blue), neutral (PAS) and Muc2 (anti-Muc2 antibody) mucins. The staining of the three mucins is lower in the reeler colon epithelium as compared with the wild-type colon (Fig. 2A). The quantification of PAS- and Muc2- positive cells (Fig. 2B) reveals that the number and maturation of goblet cells, respectively, are higher in the distal than in the proximal colon of wild-type mice and that they diminish in the reeler mice. PAS positive cells are reduced by 38 ± 5.5 % in the proximal and by 70 ± 4.8 % in the distal colon and Muc2 positive cells are reduced by 21 ± 2% in the proximal colon and by 55 ± 3% in the distal colon. The number of Alcian blue stained cells was not evaluated because of the difficulty to be counted.

As the changes induced by the mutation on cell differentiation are higher in the distal than in the proximal colon, the terminal differentiation into colonocytes and

enteroendocrine cells was evaluated only in the distal colon. Carbonic anhydrase-1 and chromogranin A were chosen as markers of colonocytes and enteroendocrine cells, respectively. Fig. 3 shows that in both, wild-type and reeler mice the carbonic anhydrase-1 positive cells are mainly located at the surface epithelium whereas the chromogranin A positive cells are dispersed within the crypts. Fig. 3 also reveals that carbonic anhydrase-1 immunostaining and the number of chromogranin A positive cells in the reeler colon is lower than in the wild-type colon. The number of enteroendocrine cells per crypt decreases by 45.5 ± 9 % in the reeler mice as compared with the wild-type mice. The number of carbonic anhydrase-1 positive cells was not evaluated because of counting difficulty.

The findings discussed so far indicate that the magnitudes of the epithelium cell renewal processes are higher in the distal than in the proximal colon and that they are decreased by the reeler mutation.

3.2. Morphology of the colon in wild-type and reeler mice

We next examined whether the changes induced by the mutation in epithelial cell proliferation, migration, differentiation and apoptosis are translated to changes in the gross morphology of the colon. The depth and diameter of the crypts were measured by light microscopy in hematoxylin and eosin stained sections of colon of 1 and 3 month-old mice. Table 2 reveals that the crypts are deeper in the distal colon than in the proximal in both, wild-type and reeler mice. The crypts diameter is significantly greater in the distal than in the proximal colon only in the three month-old wild-type mice. The reeler mutation decreases the weight and length of the colon (Fig. 4) and the depth of the crypts. The mutation significantly reduces the diameter of the crypts only in the distal colon (Table 2 and Fig. 4).

Examination at the electron microscope of the surface epithelium of distal colon reveals larger and thinner microvilli in the reeler than in the wild-type mice (Fig. 5A). The photographs also show that the tight and the adherens junctions appear normal but the intercellular space of desmosomes is significantly wider in the reeler than in the wild-type mice (Fig. 5B).

3.3. mRNA abundance of Sox9, Cdx2, Cyclin D1, Smad5, Hes1 and Atoh1 in the colon of wild-type and reeler mice with or without DSS-treatment

To get some insight into the molecular mechanisms by which reelin regulates colon epithelium homeostasis and reduces the response to experimentally induced colon pathology, we next evaluated the mRNA abundance of Sox9, Cdx2, Hes1, Atoh1, Cyclin D1 and Smad5. In the intestinal epithelium Sox9, Cdx2, Hes1 and Atoh1 control the cell proliferation, differentiation and fate decision of stem/proliferator cells to either

absorptive or secretory cells [13]. Smad5 was chosen because its absence induces modifications in the apical junctions [14] similar to those previously observed in the intestine of the reeler mice [5] and Cyclin D1 was tested because it controls cell replication [15]. The measurements were made in the distal colon of DSS-treated and untreated wild-type and reeler mice. The results in Fig. 6A reveal that under not inflammatory conditions (DSS-untreated mice) the mutation significantly decreases Sox9 and Cdx2 mRNA levels, without affecting the others genes tested, suggesting that the down-regulation of Sox9 and Cdx2 might contribute to the reeler phenotype of the colon epithelium.

The results obtained in response to DSS-treatment are given in Fig. 6B as the ratio of the mRNA levels measured in the DSS-treated *vs.* those in DSS-untreated mice. They show that DSS-treatment reduces Cdx2, Hes1 and Atoh1 mRNA levels and increases those of Sox9, but these changes are of similar magnitude in both types of mice. DSS-treatment up-regulates Smad5 and Cyclin D1 in the reeler colon, whereas in the wild-type mice, it decreases Smad5 mRNA abundance and does not change that of Cyclin D1 mRNA.

3.4. Cytokines expression in the colon of DSS-treated wild-type and reeler mice.

The mRNA abundance of the proinflammatory cytokines interleukin-6 [IL-6] and interferonγ [IFNγ] was evaluated in the DSS-treated mice colon and the results reveal that the reeler mutation increases the mRNA abundance of IL-6 from 3.3 ± 1 in wild-type to 79 ± 20 in the reeler mice ($p<0.01$, $n=5$) and decreases that of IFNγ from 35.6 ± 9 in wild-type to 2.6 ± 1 ($p<0.01$, $n=5$) in reeler mice.

3.5. AOM/DSS-induced tumour development in wild-type and reeler mice

It is well known that chronic ulcerative colitis is associated with an increased risk to develop colorectal cancer and these conditions have been reproduced in the current study to test whether reelin provides resistance to tumour development. We examined the susceptibility to colon tumorigenesis of wild-type and reeler mice subjected to AOM/DSS-treatment, as described in Methods. Both types of mice developed tumours in the distal colon with a 100% incidence and the hematoxylin and eosin stained tumour sections reveal that all the tumours analysed have adenocarcinoma appearance (Fig. 7C). The results also reveal that the reeler mice are more sensitive to colitis-associated tumorigenesis than wild-type mice, because they exhibit higher mortality during the AOM/DSS treatment (20% *vs.* 0% in wild-type mice) and increased average of tumours number and size as compared with the wild-type mice. Tumours larger than 3 mm of diameter are only observed in reeler mice (Fig. 7A and B). These

observations indicate that the reeler mutation enhances colitis-associated tumours promotion.

Discussion

Several gastrointestinal and extra-intestinal diseases have been associated with disruption of the gut barrier and we show here that reelin protection against colon pathology could be due to its contribution to the maintenance of the intestinal barrier integrity. Thus the mutation: i) decreases the magnitude of the epithelial cell proliferation, migration, differentiation and apoptosis; ii) expands the desmosomes intercellular space, and iii) decreases the length of the crypts. The decreased epithelial cell proliferation would slow epithelium renewal and even barrier restoration following injury. The diminution in goblet cells differentiation and maturation, the latter indicated by the decrease in Muc2 staining, would impair the mucus layer, and defects in renewal and formation of the inner mucus layer allow bacteria to reach the epithelium and have implications for the causes of colitis [16]. In addition, goblet cells participate in intestinal immune homeostasis by delivering low molecular weight antigens from the intestinal lumen to underlying dendritic cells [17]. The decrease in cell apoptosis would increase the exposition time of colonocytes to deleterious or mutagenic agents and therefore increase the epithelium susceptibility to damage. The mutation-induced alteration of the desmosomes might indicate disassembling of the junction, which in turn may impair the intestinal barrier [18], an effect that would be worsened by the colitis-induced neutrophil infiltration. Some studies recognize a role for the desmosomes in tumour suppression [19], in inflammatory bowel diseases development [20] and in the shape of the microvilli [21]. The physiological meaning of the mutation-induced changes in the microvilli shape is not evident, though microvilli membrane is the site of transport proteins and enzymes. Finally, the mutation-related decrease in the length of the crypts will reduce the thickness of the mucosa. All these observations indicate that the absence of reelin weakens the intestinal barrier and therefore the intestinal defense against the broad spectrum of potentially lethal microorganisms and carcinogens present in the intestinal lumen (see [1] for a review).

The current work also shows that in the wild-type mice, the magnitude of the epithelium renewal processes and the length of the crypts are in the distal colon greater than in the proximal. Similar regional differences in cell proliferation [22] and length of the crypts [23] have been reported. These regional differences might be related to their physiological functions. The distal colon absorbs fluid against a high hydraulic resistance in the lumen, whereas the proximal is unable to do this, and the larger suction tension requires longer crypts [24].

The mechanistically complex colon epithelium homeostasis, maintained by the interplay of various signalling pathways, that maintains the balance between

proliferation, differentiation and apoptosis, is still being uncovered. We have evaluated the effect of the mutation on the expression of Sox9, Cdx2, Hes1 and Atoh1, genes known to regulate the dynamics of the crypt/surface unit [13]. We found that the reeler mutation does not modify the mRNA levels of Hes1 and Atoh1 but decreases those of Sox9 and Cdx2, suggesting that the down-regulation of the two genes may contribute to establish the reeler phenotype of the colon epithelium. The observations agree with those showing variations in Sox9 expression in the same direction as epithelial cell proliferation [25–27] and goblet cells differentiation and maturation [28], and with reports revealing that Cdx2 activates genes of differentiated colonocytes, such as carbonic anhydrase-1 [29], and of differentiated goblet cells, such as Muc2 [30]. The components of the reelin signalling system have been studied intensively in the central nervous system, but, as far as we are aware, no relation between reelin and these two genes has been described with the exception of a report showing that absence of reelin decreases Sox9 expression in digit mesoderm cell cultures [31].

DSS-treatment increases Sox9 mRNA abundance and decreases that of Cdx2, Hes1 and Atoh1 to the same proportion in both types of mice, indicating that the changes are due to DSS-treatment by itself. Smad5 and Cyclin D1 were differently expressed in DSS-treated wild-type and reeler mice. DSS-treatment decreases Smad5 mRNA abundance and produces no change on that of Cyclin D1 in wild-type mice, but increases the mRNAs levels of both genes in the reeler mice, suggesting that reelin signalling represses *Smad5* and *Cyclin D1*. Recent studies have associated activation of Smad5 and Cyclin D1 with cancer. Activation of Smad5 has been observed in several cancers, including colon cancer [32]. Activation of the proto-oncogene Cyclin D1 has been found in ulcerative colitis and colorectal carcinoma [33–35] and its loss or reduction reduces intestinal tumour formation in mice carrying mutations that develop intestinal adenomas [36]. IL-6 and IFNγ were also differently expressed in both types of mice. DSS-treated reeler mice exhibit higher IL-6 mRNA levels and lower IFNγ mRNA levels than DSS-treated wild-type mice. IL-6 is a proinflammatory cytokine associated with colon cancer [37–39] and contributes to the formation of a tumour supportive microenvironment that increases the propensity of human ulcerative colitis to malignant transformation [40]. The reduced IFNγ mRNA levels observed in the reeler mice were at first unexpected because it is considered as a proinflammatory cytokine. However, IFNγ production is essential for antitumour immunity in colon [41–43]. In line with the protumorigenic phenotype observed in the reeler mice, intestinal reelin appears to be protective against tumorigenesis induced by chemical agents. Thus in response to AOM/DSS-treatment, the reeler mice colon develops higher number of tumours and of

bigger size than the wild-type. These observations agree with our previous one in human colon [7] and with that of Castellano et al. [44] showing that increased levels of reelin are related with reduced lung tumorigenesis in mice.

Together the observations suggest that reelin provides protection from worsening the acute colon inflammation and/or from progression to cancer development by reducing the response of Smad5, Cyclin D1, IL-6 and IFNγ to DSS-treatment. As reelin deletion alone is not sufficient to initiate colon pathology in the mouse, because the reeler mice remain pathology-free up to 15 months of age [5], we propose that in response to challenges, such as inflammation, reelin increases to reinforce intestinal barrier integrity, facilitate tissue repair and suppress activation of tumorigenic genes. If acute colitis progresses to conditions that reduce or suppress reelin expression, then the absence of reelin favors the formation of a tumour supportive microenvironment that would worse inflammation and/or induce tumorigenesis.

In summary, the current results highlight an essential role for reelin in maintaining intestinal epithelial cell homeostasis and providing resistance against colon pathology. They also suggest that Sox9, Cdx2, Smad5, Cyclin D1, IL-6 and IFNγ might function as downstream mediators of the reelin signalling.

Funding

The work was supported by a Grant from the Junta de Andalucía [CTS 5884] and by an associated pre-doctoral to Carvajal AE.

Conflict of interest

The authors have declared that no conflicts of interest exist.

Acknowledgements

Electronmicroscopy images were obtained in the Centro de Investigación, Tecnología e Innovación (CITIUS), Universidad de Sevilla.

References

[1] D. Viggiano, G. Ianiro, G. Vanella, S. Bibbo, G. Bruno, G. Simeone, G. Mele, Gut barrier in health and disease: focus on childhood, Eur. Rev. Med. Pharmacol. Sci. 19 (2015) 1077–1085.

[2] R.S. Sellers, D. Morton, The colon: from banal to brilliant, Toxicol. Pathol. 42 (2014) 67–81. doi:10.1177/0192623313505930.

[3] D.W. Powell, I. V Pinchuk, J.I. Saada, X. Chen, R.C. Mifflin, Mesenchymal cells of the intestinal lamina propria, Annu. Rev. Physiol. 73 (2011) 213–237. doi:10.1146/annurev.physiol.70.113006.100646.

[4] P. García-Miranda, M.J. Peral, A.A. Ilundain, Rat small intestine expresses the reelin-Disabled-1 signalling pathway, Exp. Physiol. 95 (2010) 498–507. doi:10.1113/expphysiol.2009.050682.

[5] P. García-Miranda, M.D. Vázquez-Carretero, P. Sesma, M.J. Peral, A.A. Ilundain, Reelin is involved in the crypt-villus unit homeostasis, Tissue Eng. Part A. 19 (2013) 188–98. doi:10.1089/ten.TEA.2012.0050.

[6] A.E. Carvajal, M.D. Vazquez-Carretero, P. Garcia-Miranda, M.J. Peral, M.L. Calonge, A.A. Ilundain, Reelin expression is up-regulated in mice colon in response to acute colitis and provides resistance against colitis, Biochim. Biophys. Acta. 1863 (2017) 462–473. doi:10.1016/j.bbadis.2016.11.028.

[7] J.M. Serrano-Morales, M.D. Vazquez-Carretero, M.J. Peral, A.A. Ilundain, P. Garcia-Miranda, Reelin-Dab1 signaling system in human colorectal cancer, Mol Carcinog. (2016). doi:10.1002/mc.22527.

[8] G. D'Arcangelo, G.G. Miao, S.C. Chen, H.D. Soares, J.I. Morgan, T. Curran, A protein related to extracellular matrix proteins deleted in the mouse mutant reeler, Nature. 374 (1995) 719–723. doi:10.1038/374719a0.

[9] A.E. Carvajal, A. de los Santos, M.D. Vazquez-Carretero, M.J. Peral, A.A. Ilundain, M.L. Calonge, The colon of control and reeler mice in health and disease, Acta Physiol. 212 (2014) 90.

[10] A.E. Carvajal, M.D. Vazquez-Carretero, M.J. Peral, A.A. Ilundain, M.L. Calonge, DSS-induced inflammation and regulation of reelin gene expression in mouse colon, Acta Physiol. 215 (2015) 97.

[11] J.M. Serrano-Morales, M.D. Vázquez-Carretero, A.E. Carvajal, M.L. Calonge, M.J. Peral, A.A. Ilundáin, P. García- Miranda, Reelin expression in colon cancer

progression in mice, in: J Physiol Biochem, 2016: p. 104.

[12] I. Okayasu, T. Ohkusa, K. Kajiura, J. Kanno, S. Sakamoto, Promotion of colorectal neoplasia in experimental murine ulcerative colitis., Gut. 39 (1996) 87–92.

[13] C.A. Richmond, D.T. Breault, Regulation of gene expression in the intestinal, Prog Mol Biol Transl Sci. 96 (2010) 207–229. doi:10.1016/B978-0-12-381280-3.00009-9.Regulation.

[14] J.M. Allaire, M. Darsigny, S.S. Marcoux, S. a B. Roy, J.-F. Schmouth, L. Umans, A. Zwijsen, F. Boudreau, N. Perreault, Loss of Smad5 leads to the disassembly of the apical junctional complex and increased susceptibility to experimental colitis., Am. J. Physiol. Gastrointest. Liver Physiol. 300 (2011) G586–G597. doi:10.1152/ajpgi.00041.2010.

[15] V. Baldin, J. Lukas, M.J. Marcote, M. Pagano, G. Draetta, Cyclin D1 is a nuclear protein required for cell cycle progression in G1, Genes Dev. 7 (1993) 812–821. doi:10.1101/gad.7.5.812.

[16] S.J. Chen, X.W. Liu, J.P. Liu, X.Y. Yang, F.G. Lu, Ulcerative colitis as a polymicrobial infection characterized by sustained broken mucus barrier, World J. Gastroenterol. 20 (2014) 9468–9475. doi:10.3748/wjg.v20.i28.9468.

[17] J.R. McDole, L.W. Wheeler, K.G. McDonald, B. Wang, V. Konjufca, K.A. Knoop, R.D. Newberry, M.J. Miller, Goblet cells deliver luminal antigen to CD103+ dendritic cells in the small intestine, Nature. 483 (2012) 345–9. doi:10.1038/nature10863.

[18] N. Schlegel, M. Meir, W.-M. Heupel, B. Holthofer, R.E. Leube, J. Waschke, Desmoglein 2-mediated adhesion is required for intestinal epithelial barrier integrity., Am. J. Physiol. Gastrointest. Liver Physiol. 298 (2010) G774–83. doi:10.1152/ajpgi.00239.2009.

[19] R.L. Dusek, L.D. Attardi, Desmosomes: new perpetrators in tumour suppression, Nat. Rev. Cancer. 11 (2011) 317–323. doi:10.1038/nrc3051.

[20] N. Gassler, C. Rohr, a Schneider, J. Kartenbeck, a Bach, N. Obermüller, H.F. Otto, F. Autschbach, Inflammatory bowel disease is associated with changes of enterocytic junctions, Am. J. Physiol. Gastrointest. Liver Physiol. 281 (2001) G216–G228.

[21] K.D. Sumigray, T. Lechler, Desmoplakin controls microvilli length but not cell adhesion or keratin organization in the intestinal epithelium, Mol. Biol. Cell. 23

(2012) 792–9. doi:10.1091/mbc.E11-11-0923.

[22] T. Inoue, M. Murano, T. Kuramoto, K. Ishida, K. Kawakami, Y. Abe, E. Morita, N. Murano, K. Toshina, T. Nishikawa, K. Maemura, C. Shimamoto, I. Hirata, K.I. Katsu, K. Higuchi, Increased proliferation of middle to distal colonic cells during colorectal carcinogenesis in experimental murine ulcerative colitis, Oncol. Rep. 18 (2007) 1457–1462.

[23] P.A. Neumann, S. Koch, R.S. Hilgarth, E. Perez-Chanona, P. Denning, C. Jobin, A. Nusrat, Gut commensal bacteria and regional Wnt gene expression in the proximal versus distal colon, Am. J. Pathol. 184 (2014) 592–599. doi:10.1016/j.ajpath.2013.11.029.

[24] R.J. Naftalin, K.C. Pedley, Regional crypt function in rat large intestine in relation to fluid absorption and growth of the pericryptal sheath, J. Physiol. 514 (1999) 211–227. doi:10.1111/j.1469-7793.1999.211af.x.

[25] B.B. McConnell, S.S. Kim, K. Yu, A.M. Ghaleb, N. Takeda, I. Manabe, A. Nusrat, R. Nagai, V.W. Yang, Krppel-like factor 5 is important for maintenance of crypt architecture and barrier function in mouse intestine, Gastroenterology. 141 (2011). doi:10.1053/j.gastro.2011.06.086.

[26] A. Matheu, M. Collado, C. Wise, L. Manterola, L. Cekaite, A.J. Tye, M. Canamero, L. Bujanda, A. Schedl, K.S.E. Cheah, R.I. Skotheim, R.A. Lothe, A.L. De Munain, J. Briscoe, M. Serrano, R. Lovell-Badge, Oncogenicity of the developmental transcription factor Sox9, Cancer Res. 72 (2012) 1301–1315. doi:10.1158/0008-5472.CAN-11-3660.

[27] S. Liu, Y. Qian, L. Li, G. Wei, Y. Guan, H. Pan, X. Guan, L. Zhang, X. Lu, Y. Zhao, M. Liu, D. Li, Lgr4 gene deficiency increases susceptibility and severity of dextran sodium sulfate-induced inflammatory bowel disease in mice, J. Biol. Chem. 288 (2013) 8794–8803. doi:10.1074/jbc.M112.436204.

[28] P. Bastide, C. Darido, J. Pannequin, R. Kist, S. Robine, C. Marty-Double, F. Bibeau, G. Scherer, D. Joubert, F. Hollande, P. Blache, P. Jay, Sox9 regulates cell proliferation and is required for Paneth cell differentiation in the intestinal epithelium, J. Cell Biol. 178 (2007) 635–648. doi:10.1083/jcb.200704152.

[29] F.J. Drummond, J. Sowden, K. Morrison, Y.H. Edwards, Colon carbonic anhydrase 1: Transactivation of gene expression by the homeodomain protein Cdx2, FEBS Lett. 423 (1998) 218–222. doi:10.1016/S0014-5793(98)00103-3.

[30] H. Yamamoto, Y.Q. Bai, Y. Yuasa, Homeodomain protein CDX2 regulates

goblet-specific MUC2 gene expression, Biochem. Biophys. Res. Commun. 300 (2003) 813–818. doi:10.1016/S0006-291X(02)02935-2.

[31] M.J. Diaz-Mendoza, C.I. Lorda-Diez, J.A. Montero, J.A. Garcia-Porrero, J.M. Hurle, Reelin/DAB-1 signaling in the embryonic limb regulates the chondrogenic differentiation of digit mesodermal progenitors, J. Cell. Physiol. 229 (2014) 1397–1404. doi:10.1002/jcp.24576.

[32] J. Ke, J. Lou, X. Chen, J. Li, C. Liu, Y. Gong, Y. Yang, Y. Zhu, Y. Zhang, J. Tian, J. Chang, R. Zhong, J. Gong, X. Miao, Identification of a functional variant for colorectal cancer risk mapping to chromosome 5q31.1., Oncotarget. (2016). doi:10.18632/oncotarget.9298.

[33] J. Bartkova, J. Lukas, M. Strauss, J. Bartek, The PRAD-1/cyclin D1 oncogene product accumulates aberrantly in a subset of colorectal carcinomas, Int. J. Cancer. 58 (1994) 568–573. doi:10.1002/ijc.2910580420.

[34] T. Sutter, S. Doi, K.A. Carnevale, N. Arber, I.B. Weinstein, Expression of cyclins D1 and E in human colon adenocarcinomas, J. Med. 28 (1997) 285–309.

[35] N.A.C.S. Wong, N.J. Mayer, C.E. Anderson, H.C. McKenzie, R.G. Morris, J. Diebold, D. Mayr, I.W. Brock, J.A. Royds, H.M. Gilmour, D.J. Harrison, Cyclin D1 and p21 in ulcerative colitis-related inflammation and epithelial neoplasia: a study of aberrant expression and underlying mechanisms, Hum. Pathol. 34 (2003) 580–588.

[36] J. Hulit, C. Wang, Z. Li, C. Albanese, M. Rao, D. Di Vizio, S. Shah, S.W. Byers, R. Mahmood, L.H. Augenlicht, R. Russell, R.G. Pestell, Cyclin D1 genetic heterozygosity regulates colonic epithelial cell differentiation and tumor number in ApcMin mice, Mol. Cell. Biol. 24 (2004) 7598–611. doi:10.1128/MCB.24.17.7598-7611.2004.

[37] Y.-C. Chung, Y.-F. Chang, Serum interleukin-6 levels reflect the disease status of colorectal cancer, J. Surg. Oncol. 83 (2003) 222–226. doi:10.1002/jso.10269.

[38] G. Galizia, M. Orditura, C. Romano, E. Lieto, P. Castellano, L. Pelosio, V. Imperatore, G. Catalano, C. Pignatelli, F. De Vita, Prognostic significance of circulating IL-10 and IL-6 serum levels in colon cancer patients undergoing surgery, Clin. Immunol. 102 (2002) 169–178. doi:10.1006/clim.2001.5163.

[39] C. Becker, M.C. Fantini, C. Schramm, H.A. Lehr, S. Wirtz, A. Nikolaev, J. Burg, S. Strand, R. Kiesslich, S. Huber, H. Ito, N. Nishimoto, K. Yoshizaki, T. Kishimoto, P.R. Galle, M. Blessing, S. Rose-John, M.F. Neurath, TGF-beta

suppresses tumor progression in colon cancer by inhibition of IL-6 trans-signaling, Immunity. 21 (2004) 491–501. doi:10.1016/j.immuni.2004.07.020.

[40] Y. Li, J. Deuring, M.P. Peppelenbosch, E.J. Kuipers, C. de Haar, C.J. van der Woude, IL-6-induced DNMT1 activity mediates SOCS3 promoter hypermethylation in ulcerative colitis-related colorectal cancer, Carcinogenesis. 33 (2012) 1889–1896. doi:10.1093/carcin/bgs214.

[41] B. Sharma, R. V Iozzo, Transcriptional silencing of perlecan gene expression by interferon-gamma, J. Biol. Chem. 273 (1998) 4642–4646. doi:10.1074/jbc.273.8.4642.

[42] P. Sundström, F. Ahlmanner, P. Akéus, M. Sundquist, S. Alsén, U. Yrlid, L. Börjesson, Å. Sjöling, B. Gustavsson, S.B.J. Wong, M. Quiding-Järbrink, Human Mucosa-Associated Invariant T Cells Accumulate in Colon Adenocarcinomas but Produce Reduced Amounts of IFN-γ, J. Immunol. 195 (2015) 3472–3481. doi:10.4049/jimmunol.1500258.

[43] L. Wang, Y. Wang, Z. Song, J. Chu, X. Qu, Deficiency of interferon-gamma or its receptor promotes colorectal cancer development, J. Interferon Cytokine Res. 35 (2015) 273–80. doi:10.1089/jir.2014.0132.

[44] E. Castellano, M. Molina-Arcas, A.A. Krygowska, P. East, P. Warne, A. Nicol, J. Downward, RAS signalling through PI3-Kinase controls cell migration via modulation of Reelin expression, Nat. Commun. 7 (2016) 1–112. doi:10.1038/pj.2016.37.

Legends

Fig. 1. Cell proliferation, migration and apoptosis in colon epithelium of wild-type and reeler mice. 7 µm cryosections of the colon were obtained from 1 month-old wild-type and reeler mice. The sections were immunostained with anti-BrdU antibody (1:300 dilution) for proliferation [A] and migration [B] assays and with anti-caspase 3 antibody (1:200 dilution) for apoptosis measurements [C]. Mice were killed either 90 min or 15 h after BrdU injection for cell proliferation and migration measurements, respectively. In B, lines indicate the front point of labelled cells used to evaluate cell migration rate, expressed in µm/h. In C, arrows indicate caspase 3 labelled cells. Scale bar represents 50 µm. The number of BrdU-labelled cells was determined in 30 crypts and those labelled with anti-caspase 3 antibody in 150 crypts per mouse. Histograms represent means ± SEM. Five reeler and five wild-type mice were used. One-way ANOVA showed an effect of mutation and colon region on the cell proliferation, migration and apoptosis ($p<0.001$). Newman-Keuls' test: *$p<0.001$ reeler *vs*. wild-type mice and $^{\#}p<0.001$ distal *vs*. proximal colon.

Fig. 2. Number and maturation of goblet cells in colon epithelium of wild-type and reeler mice. 5 µm paraffin-embedded colon sections of 1 month-old wild-type and reeler mice were stained for acidic, neutral and Muc2 mucins with Alcian blue, PAS and anti-Muc2 antibody (1:50 dilution), respectively. A, Representative stained goblet cells in the distal colon are shown. Scale bar = 50 µm. B, Histograms represent means ± SEM of the number of PAS- and Muc2-positive cells per crypt. Five reeler and five wild-type mice were used. One-way ANOVA showed an effect of mutation on the cell differentiation and maturation of goblet cells and colon region ($p<0.001$). Newman-Keuls' test: *$p<0.001$ reeler *vs*. wild-type mice and $^{\#}p<0.001$ distal *vs*. proximal colon.

Fig. 3. Cell differentiation into colonocytes and enteroendocrine cells in wild-type and reeler mice. 5 µm paraffin colon sections were immunostained for carbonic anhydrase-1 and chromogranin A using anti-carbonic anhydrase-1 (1:50 dilution) and anti-chromogranin A (1:100 dilution) antibodies, respectively. Arrows indicate labelled cells. Representative specimens are shown. Scale bar = 50 µm. Histogram represents means ± SEM of the number of enteroendocrine labelled cells per crypt. Five reeler and five wild-type mice were used. Student's *t* test: *$p<0.001$ reeler *vs.* wild-type mice.

Fig. 4. Colon weight and length of wild-type and reeler mice. 1 month and 3 month-old wild-type and reeler mice were used. Data are presented as the means ± SEM of five different animals per age and type of mouse. The photograph represents the cecum and colon of wild-type and reeler mice. Blue, red and green lines represent the length

of the cecum, proximal and distal colon, respectively. One-way ANOVA showed an effect of mutation on colon weight and length ($p<0.001$). Newman-Keuls' test: *$p<0.001$ and **$p<0.01$ reeler *vs.* wild-type mice.

Fig. 5. Electron microscopy of the apical domain of control and reeler colon epithelium. A, Microvilli (M) of colon epithelium are shown. Scale bar = 1000 nm. B, Apical cell-to-cell junctions. TJ, tight junction; AJ, adherens junction; D, desmosome. 25 to 30 junctions were examined per type of mouse. Scale bar = 200 nm. The histograms represent means ± SEM of microvilli width or length, and of junction width. The microphotographs are representative of three different assays performed on five reeler and five wild-type mice of 3 month-old. Student's t test: *$p<0.001$ reeler *vs.* wild-type mice.

Fig. 6. mRNA levels of Sox9, Cyclin D1, Cdx2, Smad5, Hes1 and Atoh1 in the colon epithelium of wild-type and reeler mice with or without DSS-treatment. Mice of 3 month-old received 3% DSS in the drinking water during 9 days, as described in Methods. A, mRNA relative abundance in DSS-untreated wild-type and reeler mice. B, The histograms represent the mRNA abundance fold change produced by DSS-treatment relative to DSS-untreated-mice. Data are means ± SEM. The number of animals used was five reeler and five wild-type mice. One way ANOVA revealed an effect of the mutation and of DSS-treatment on mRNA abundance of the genes tested ($p<0.001$). Newman-Keuls´ test: $^{a}p<0.001$ and $^{b}p<0.01$ DSS-treated *vs*. untreated mice; *$p<0.01$, **$p<0.05$ reeler *vs*. wild-type mice.

Fig. 7. Evaluation of the colitis-associated tumorigenesis in wild-type and reeler mice. Mice of 3 month-old received a single intraperitoneal administration of 10 mg AOM / kg of body weight followed by oral administration of DSS in the drinking water as described in Methods. Five reeler and five wild-type mice were used. A, Representative view of colons; asterisks indicate the tumours. Scale bar represents 1 cm. B, Number of tumours per mouse (Left) and number of tumours categorized by size (Right) at the end of the AOM/DSS treatment. Means ± SEM. Student's t test: *$p<0.05$ reeler *vs*. wild-type mice. C, Paraffin-embedded colon specimens were stained with hematoxylin and eosin and observed by light microscopy. Scale bar represents 100 µm.

Figure1

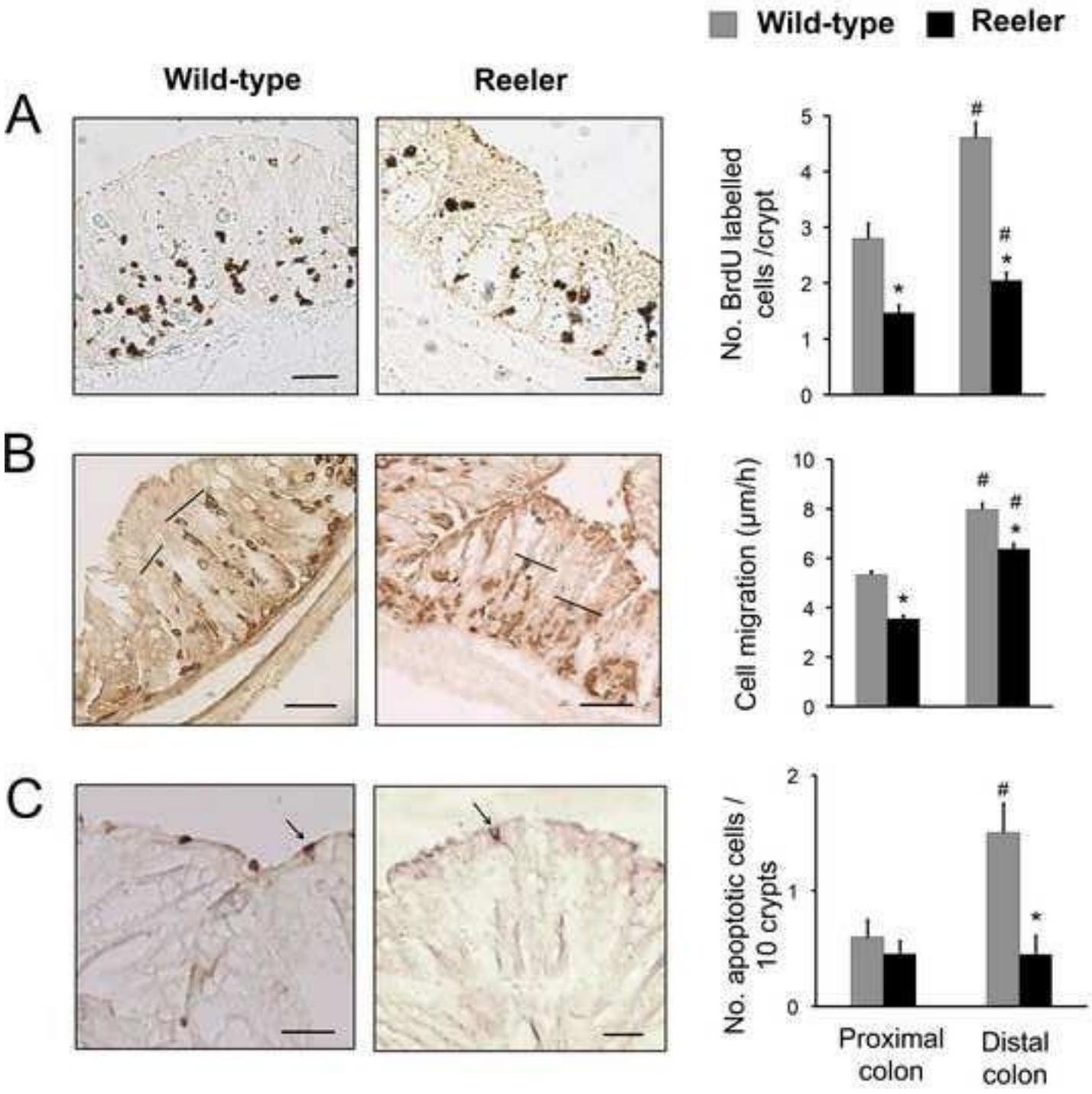
Wild-type
Reeler
A
Wild-type
Reeler
No. BrdU labelled cells /crypt
B
Cell migration (μm/h)
C
No. apoptotic cells / 10 crypts
Proximal colon
Distal colon

Figure2

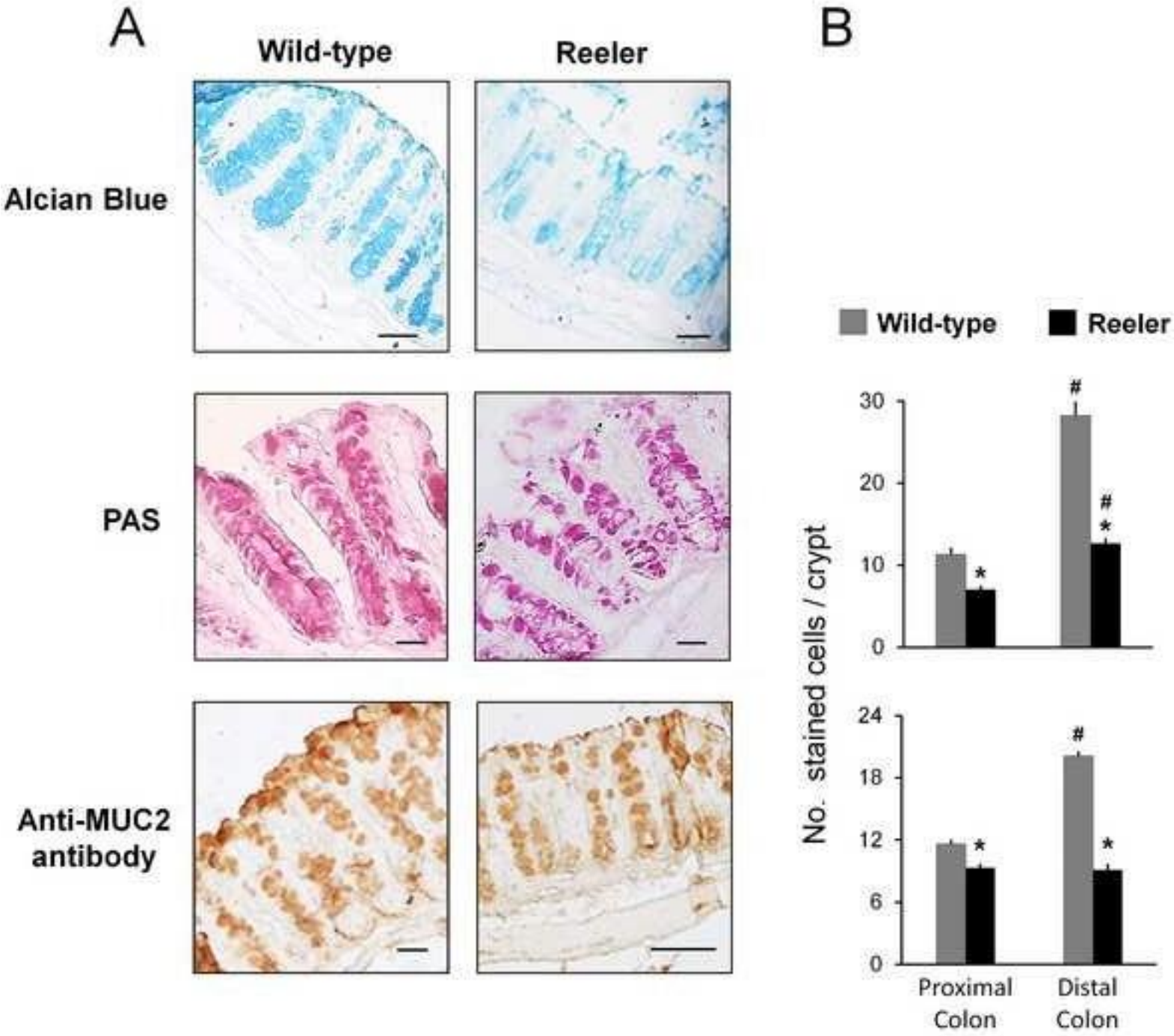
A
Wild-type
Reeler
Alcian Blue
PAS
Anti-MUC2 antibody
B
Wild-type
Reeler
No. stained cells / crypt
30
20
10
0
24
18
12
6
0
#
*
Proximal Colon
Distal Colon

Figure3

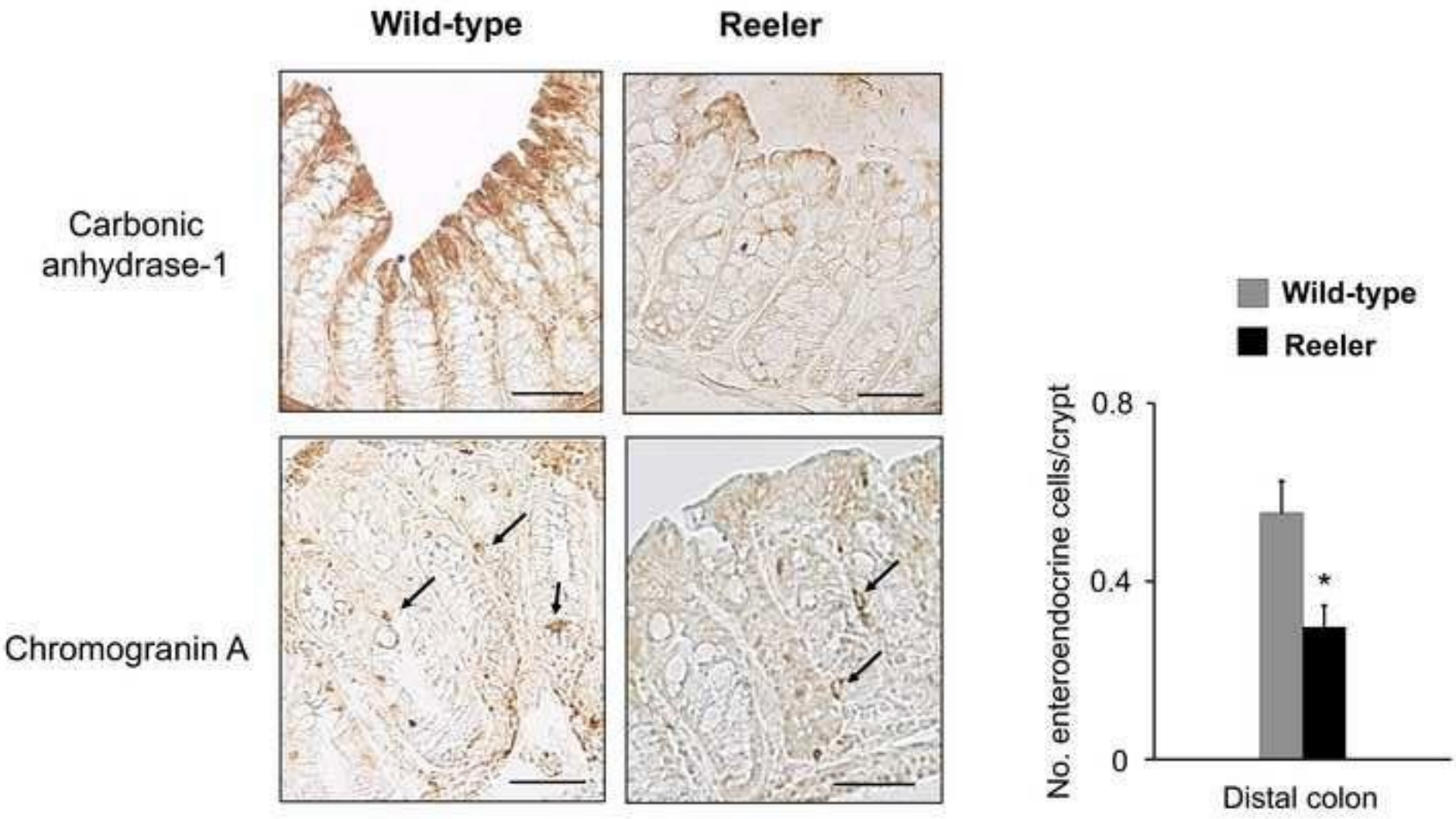
Wild-type
Reeler
Carbonic anhydrase-1
Chromogranin A
Wild-type
Reeler
No. enteroendocrine cells/crypt
0.8
0.4
0
*
Distal colon

Figure4

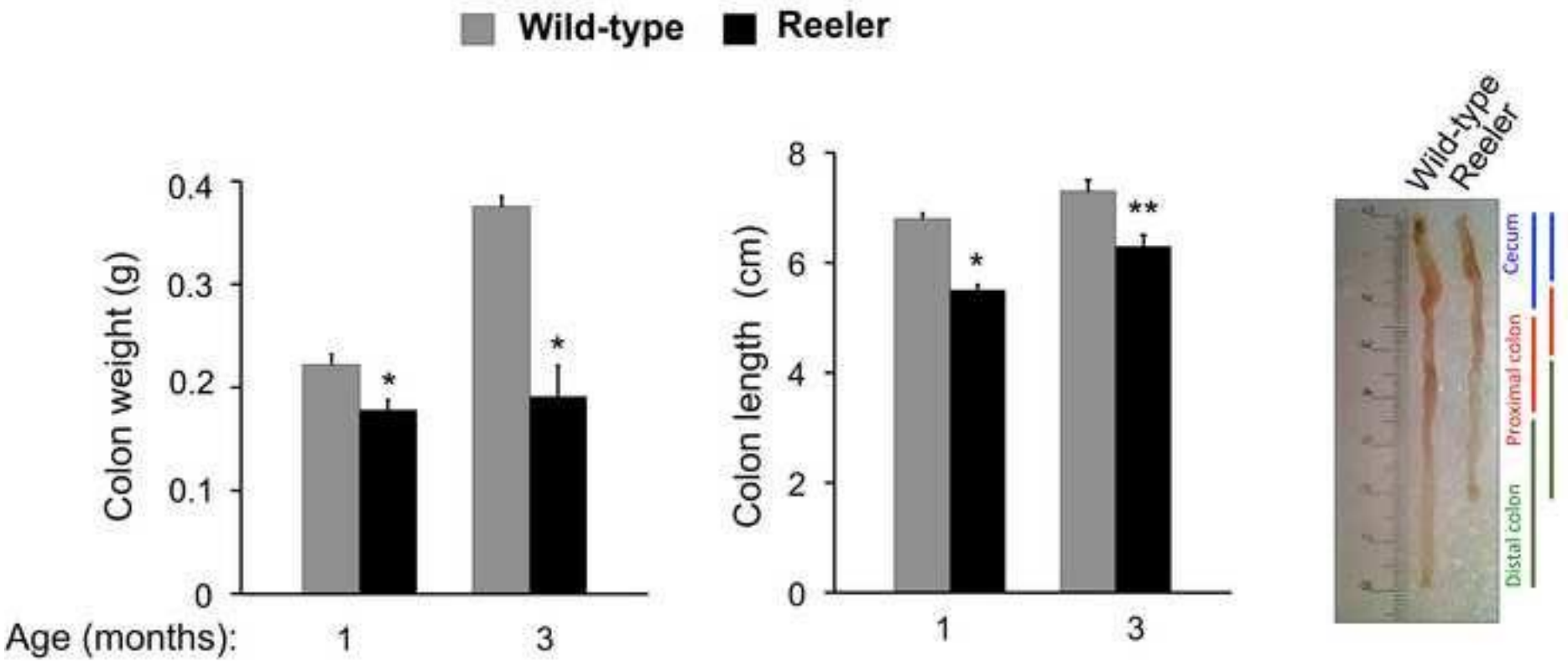
Wild-type
Reeler
Colon weight (g)
0.4
0.3
0.2
0.1
0
*
*
Age (months):
1
3
Colon length (cm)
8
6
4
2
0
*
**
1
3
Wild-type
Reeler
Cecum
Proximal colon
Distal colon

Figure5

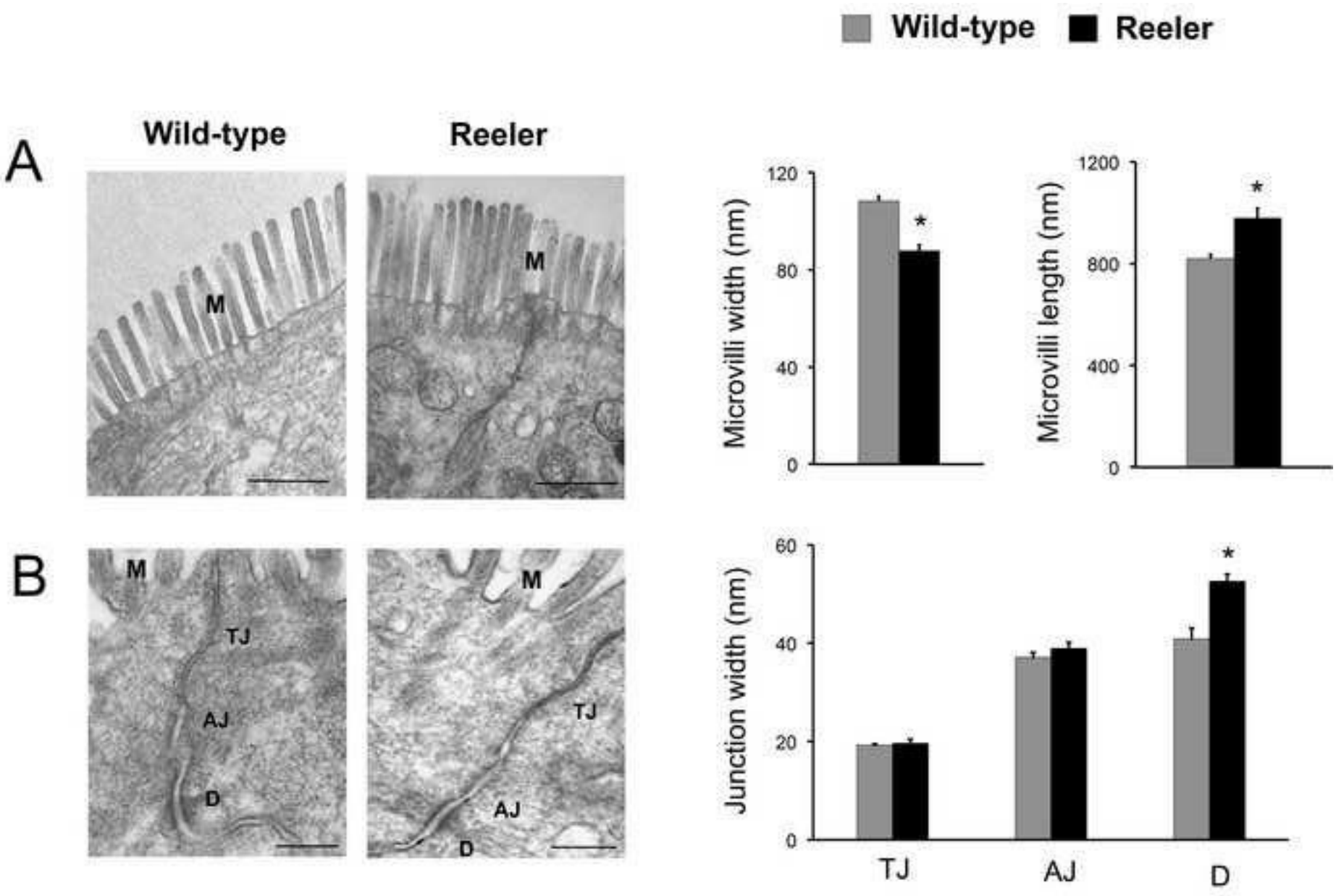
Wild-type
Reeler
A
M
M
B
M
TJ
AJ
D
M
TJ
AJ
D
Wild-type
Reeler
Microvilli width (nm)
120
80
40
0
*
Microvilli length (nm)
1200
800
400
0
*
Junction width (nm)
60
40
20
0
*
TJ
AJ
D

Figure6

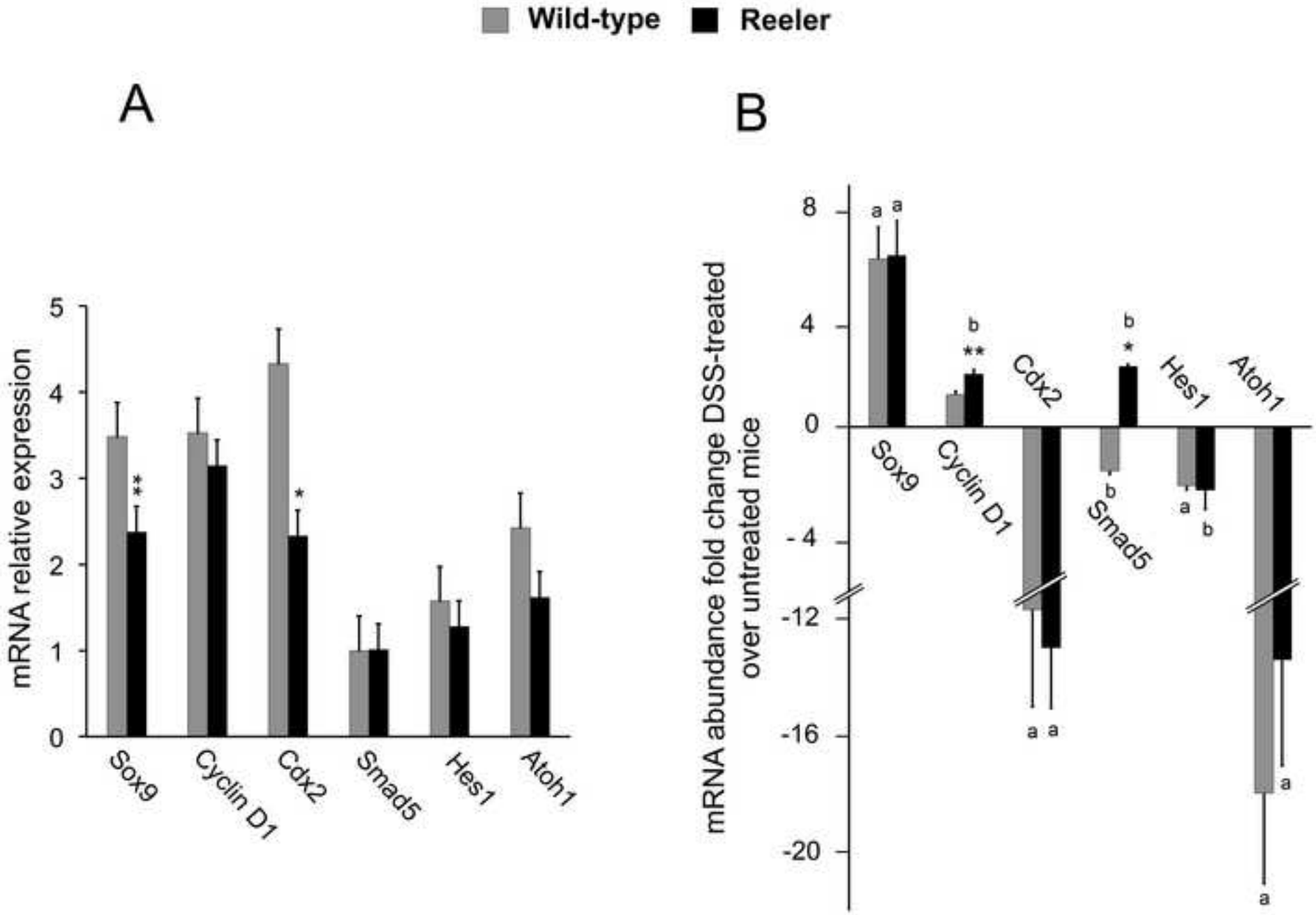
Wild-type
Reeler
A
mRNA relative expression
0
1
2
3
4
5
**
*
Sox9
Cyclin D1
Cdx2
Smad5
Hes1
Atoh1
B
mRNA abundance fold change DSS-treated over untreated mice
8
4
0
- 4
-12
-16
-20
a a
b
**
b
*
a a
b
a
b
a
Sox9
Cyclin D1
Cdx2
Smad5
Hes1
Atoh1

Figure7

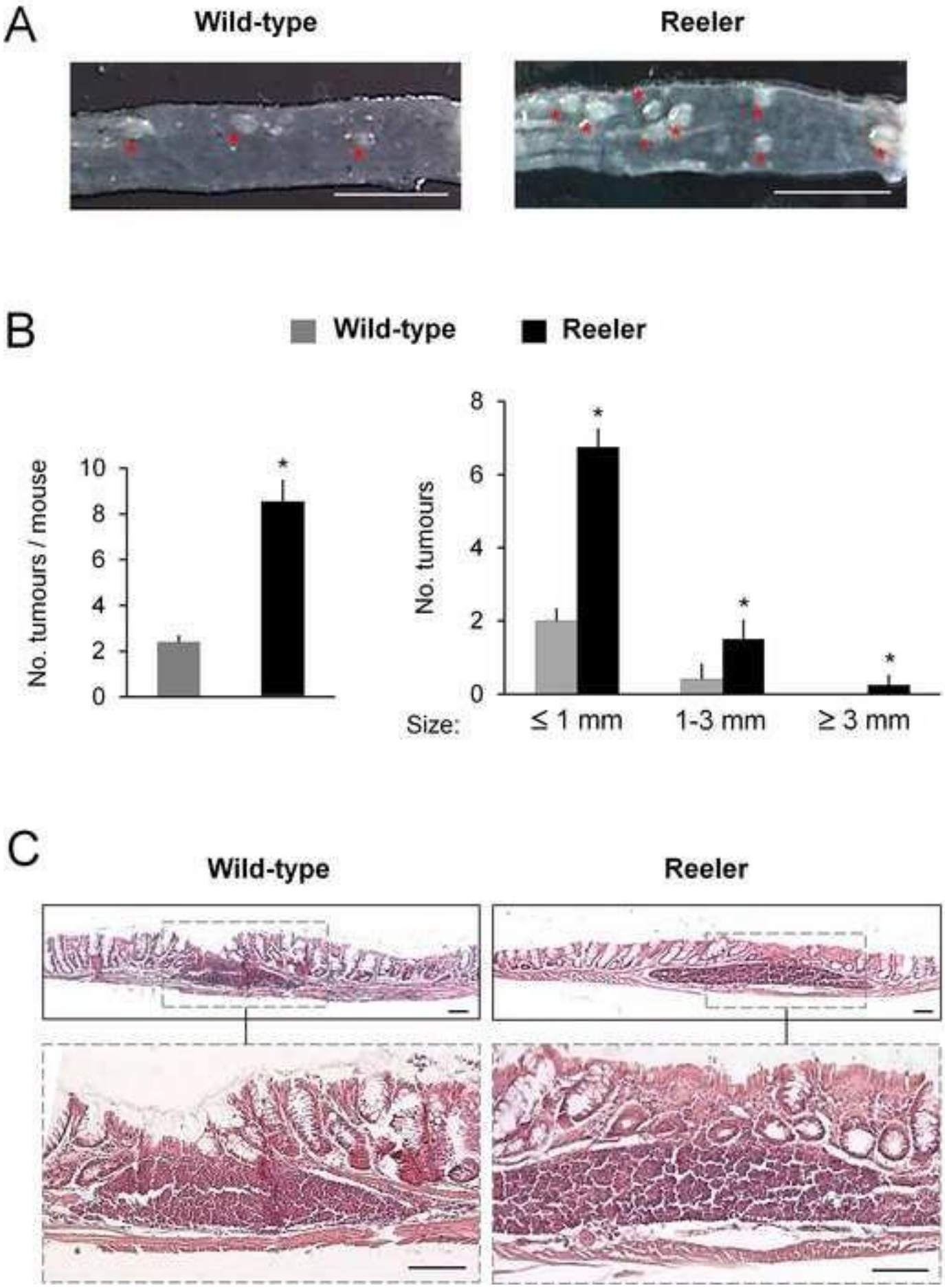
A
Wild-type
Reeler
B
Wild-type
Reeler
No. tumours / mouse
10
8
6
4
2
0
*
No. tumours
8
6
4
2
0
*
*
*
Size:
≤ 1 mm
1-3 mm
≥ 3 mm
C
Wild-type
Reeler

Table 1. Oligonucleotides sequences used for real time PCR.

Gene	Accession no.	Sense (5'- 3')	Antisense (5'- 3')
β-actin	NM_007393	ACCCACACTGTGCCCATCTA	CGGAACCGCTCATTGCC
Atoh1	NM_007500	GTATCTGCTGCATTCTCCCGA	CAAGCTCGTCCACTACAACC
Cdx2	NM_007673	AACTACAGGAGCCAGAGGCA	AGGGACAGGAAGTCCAGGTT
Cyclin D1	NM_007631	AGGCTACAGAAGAGTATTTATGGGAA	TGCGTTTGAATCAAGGGAGAT
Hes1	NM_008235	TCAACACGACACACGGACAAACC	GGTACTTCCCCAACACGCTCG
IFNγ	NM_008337	CAGCAACAGCAAGGCGAAA	CTGGACCTGTGGGTTGTTGAC
IL-6	NM_031168	ACAAGTCGGAGGCTTAATTACACAT	TTGCCATTGCACAACTCTTTTC
Smad5	NM_021692	GACAGCAGCATCTTTGTTCAG	ATCCATGGTTGACTGACTGAG
Sox9	NM_011448	TCGTGTGTGTGTGTTTATAG	ATTCCTATTGCTACACTCAG

Oligonucleotides were chosen according to cDNA sequences entered in GenBank and designed using PerlPrimer program v1.1.14. Atoh1, Atonal homolog-1; Cdx2, Caudal-type homeobox transcription factor 2; Hes1, Hairy and enhancer of split-1; IFNγ, Interferon γ; IL-6, Interleukin-6; Smad5, Mothers against decapentaplegic, drosophila, homolog of, 5; Sox9, SRY-related HMG-box, gene 9.

Table 2. Morphometric parameters of wild-type and reeler mice colon.

Mice	Crypt depth		Crypt diameter	
	Proximal	Distal	Proximal	Distal
1 month-old				
Wild-type:	93.3 ± 3	165.1 ± 3$^{\#}$	29.8 ± 1	32.1 ± 1.8
Reeler:	78.8 ± 2*	132.8 ± 3*$^{\#}$	29.1 ± 0.8	25.6 ± 1.1*
3 month-old				
Wild-type:	126.3 ± 6	251.9 ± 12$^{\#}$	36.5 ± 1.9	47.0 ± 1.3$^{\#}$
Reeler:	87.6 ± 2.5*	183.6 ± 3.4*$^{\#}$	36.2 ± 1.8	37.6 ± 1.2*

Means ± SEM of colon measurements (in µm). Five reeler and five wild-type mice per age were used. One-way ANOVA showed an effect of the colon region and mutation on colon morphology ($p<0.001$). Newman-Keuls' test: *$p<0.001$ reeler *vs.* wild-type mice; $^{\#}p<0.001$ proximal *vs.* distal colon.